A R C H I V E S O F M E T A L L U R G Y A N D M A T E R I A L S
Volume 51 2006 Issue 1

Z. KALICKA*, J. WYPARTOWICZ*

MODELLING OF INTERACTIONS BETWEEN OXIDE INCLUSION PARTICLES AT THE SLAG-METAL INTERFACE

MODELOWANIE ODDZIAŁYWAŃ MIĘDZY CZĄSTKAMI WYDZIELEŃ TLENKOWYCH NA POWIERZCHNI MIĘDZYFAZOWEJ ŻUŻEL-METAL

The values of attractive forces acting between two spherical oxide particles placed at interphase surface liquid metal – liquid slag were calculated by means of the model of capillary interaction. The problem regards the particles of the dimensions in the range between several μm and several tens of μm, and is related to the mechanism of oxide precipitates coagulation in liquid steel. It was found that in the case under consideration the attractive force is in the range 10^{-18} – 10^{-20} N and it depends mainly on the particle dimensions and the surface properties in the system: solid particle – liquid metal – liquid slag, which are represented with the contact angle.

Keywords: steel, slag, oxide inclusions, attractive force, surface capillary effect

Przy pomocy modelu oddziaływania kapilarnego wyznaczono wielkość siły przyciągającej działającej pomiędzy dwoma stałymi cząstkami tlenkowymi o kształcie kulistym, zlokalizowanymi na powierzchni międzyfazowej ciekły metal – ciekły żużel. Problem dotyczy cząstek wielkości kilku – kilkudziesięciu μm i odnosi się do mechanizmu koagulacji wydzieleń tlenkowych w ciekłej stali. Stwierdzono, że w takim przypadku wielkość siły przyciągającej jest rzędu 10^{-18} – 10^{-20} N i że zależy ona w głównej mierze od wielkości cząstek oraz własności powierzchniowych w układzie: stała cząstka – ciekły metal – ciekły żużel, wyrażających się kątem kontaktu.

1. Introduction

Non-metallic inclusions in liquid steel, which are predominantly the result of deoxidation are so far unavoidable in conventional technologies. Their amount in 1 kg of good quality steel is up to 10^9. Due to their negative influence on mechanical properties and corrosion susceptibility the operations of inclusions removal are still intensely developed. Their flotation to the slag-metal interface and formation of bigger agglomerates are the main steps in steel refinement. Deeper insight into the nature of agglomeration was possible only in recent years, when appropriate experimental techniques, mainly confocal scanning laser microscopy, became available.

The particles may form the aggregates as a results of collisions in the bulk of liquid metals due to the:

- Brownian motions,
- Differences in the floating velocity (bigger particles float with higher rate),
- Turbulent collisions.

Another mechanism of aggregation is active at the liquid steel surface. It is caused by the capillary attraction of particles. This phenomenon occurs not only at the surface of steel bath, but also inside the bubbles of inert (argon) or reductive (CO) gas, passing through the melt. This case is even more important in inclusions removal.

Experimental observations of Yin *et al.* [1, 2] and Nakajima and Mizoguchi [3] revealed that oxide particles floating on the molten steel surface may attract each other from the distance which is much bigger than their diameter. This promotes clustering and agglomeration. The semi-quantitative analysis of Yin *et al.* [1, 2] leads to the following conclusions:

- The attractive forces acting between solid alumina inclusions are of the order 10^{-16} N and can operate at the distance of 50 μm. The values of such forces may be estimated from the measurements of particles acceleration.
- As a result of attraction the alumina agglomerates of dimensions exceeding 100 μm may be formed.

* FACULTY OF METALS ENGINEERING AND INDUSTRIAL COMPUTER SCIENCE, AGH UNIVERSITY OF SCIENCE AND TECHNOLOGY, 30-059 KRAKÓW, AL. MICKIEWICZA 30, POLAND

♦ No attraction was observed within the couple solid-liquid particles. The agglomeration occurs only, if the particles are put into close contact due to steel flow.

♦ The liquid particles indicate weak attraction.

However, in the real steelmaking processes the liquid steel is covered with oxide slag layer. The direct observations of inclusions agglomeration in such a case is very difficult. Coletti et al. [4] as well as Vantilt et al. [5] observed the actual behaviour of inclusions at the metal-slag interface as well as their mutual positions in the quenched samples. It is generally agreed that the forces acting between inclusion particles are of capillary character [1-5].

The particles deform the liquid steel surface, what creates the attractive or repulsive force between particles. In order to strictly calculate this force, the shape of surface in the vicinity of particles has to be determined, i.e. the Laplace equation solved. This is generally a second-order non linear partial differential equation. Procedure developed by Kralchevsky, Paunov et al. [6, 7] offers the asymptotic solution to this equation. The original version of this procedure have been adopted by Nakajima and Mizoguchi to the case of the metal-gas surface [3]. Present work considers, however, the case of inclusions particles at the liquid steel-liquid slag interface. Its aim is to determine the difference between both types of inter-particle interaction, at the metal-gas and metal-slag interfaces.

2. Model of inter-particle capillary interaction

The system under consideration, similar to this discussed by Paunov et al [6] and Nakajima and Mizoguchi [3], consists of two spherical particles of radii R_k with the fragment of neighbouring metal-slag interface, as presented in Fig. 1. For convenience the particles are indexed k ($k = 1$ *or* 2). The particles are partly immersed in metallic (m) phase, and partly in the slag (s) phase. The inter-particle distance is L. In the system under consideration the inclusions material density ρ_k is higher than liquid slag density ρ_s and lower than metal density ρ_m. The lines at which three phases meet are the circles of radii r_k, provided that the meniscus deformation is small. At some larger distance from the particles the metal-slag interface is horizontal and flat.

The interaction between slag-metal interface and the particles results in the deformation of the shape of meniscus. The actual shape of meniscus may be described with the $z(x, y)$ function. The angle of meniscus slope at the line of three phase contact is ψ_k. If the interface is deformed in upward direction, ψ_k is given a positive value; in opposite case ψ_k is negative. The three-phase contact angle α_k is always positive.

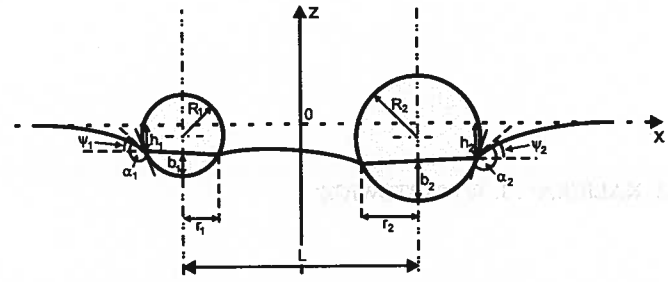

Fig. 1. Schematic diagram of two particles attracting due to the capillary forces

The total energy of the system under consideration is a sum of three contributions: gravitational, wetting and liquid meniscus:

$$W = W_g + W_w + W_m \tag{1}$$

Gravitational contribution W_g is the potential energy in the system containing the particles of mass m_k as well as appropriate masses of metal (m_m) and slag (m_s)

$$W_g = g \cdot \sum_{k=1}^{2} m_k \cdot z_k^0 + m_m \cdot g \cdot z_m^0 + m_s \cdot g \cdot z_s^0, \tag{2}$$

where z_k^0, z_m^0 and z_s^0 denote the position of the centres of corresponding masses along the coordinate, and g – the acceleration of gravity. The choice of m_m and m_s does not affect the results of calculations.

The surface free energy is the sum of interactions between particles and corresponding liquid phases:

$$W_w = \sum_{k=1}^{2} \omega_{k-m} \cdot A_{k-m} + \sum_{k=1}^{2} \omega_{k-s} \cdot A_{k-s}, \tag{3}$$

where ω_{k-m} and ω_{k-s} denote the surface energy density for the interface between particle k and metallic and slag phase, respectively, while A_{k-m} and A_{k-s} – the areas of these interfaces.

The liquid meniscus energy is:

$$W_m = \gamma \cdot \Delta A \tag{4}$$

where γ denotes the slag-metal interfacial tension, and ΔA is the difference between the area of actual metal-slag interface and its projection on horizontal plane xy.

The energy of the system has to be expressed in terms of materials properties and geometric dimensions of the system, under the condition resulting from the vertical forces balance. The force due to the surface tension must balance the gravity force F_k^g (including buoyancy)

$$2\pi \cdot \gamma \cdot r_k \cdot \sin\psi_k = F_k^g \tag{5}$$

$$F_k^g = g \cdot V_k^m \cdot (\rho_m - \rho_k) + g \cdot V_k^s \cdot (\rho_s - \rho_k) - \\ - \pi \cdot r_k^2 \cdot h_k \cdot (\rho_m - \rho_s) \tag{6}$$

where: V_k^m – part of particle volume submerged in metal,
V_k^s – part of particle volume submerged in slag,
h_k – elevation of meniscus at three phase contact line.

Total volume of particle V_k is:

$$V_k = V_k^m + V_k^s \tag{7}$$

Introducing the density factor D_k:

$$D_k = \frac{\rho_k - \rho_s}{\rho_m - \rho_s}, \tag{8}$$

one arrives at the relation:

$$F_k^g = \gamma \cdot q^2 \cdot \left(V_k^s - D_k \cdot V_k - \pi \cdot r_k^2 \cdot h_k\right), \tag{9}$$

where:

$$q = \left[\frac{(\rho_m - \rho_s) \cdot g}{\gamma}\right]^{\frac{1}{2}}. \tag{10}$$

The value of q^{-1} is termed the capillary length, as it characterizes the range of capillary interaction. For water–air system $q^{-1} \cong 2.7mm$, while in the steel-slag system $q^{-1} \cong 18mm$. The calculations in the present work are carried out under assumption of small particles size: $(q \cdot R_k)^2 << 1$.

The final results drawn from the balance of vertical forces acting on single particle are presented with the use of so called "capillary charge" of particle Q_k (Paunov *et al.* [6]). It is defined as:

$$Q_k = r_k \cdot \sin\psi_k \tag{11}$$

$$Q_k = \frac{1}{2} \cdot q^2 \cdot \left[b_k^2 \cdot \left(R_k - \frac{b_k}{3}\right) - \frac{4}{3} \cdot D_k \cdot R_k^3 - r_k^2 \cdot h_k\right], \tag{12}$$

where b_k denotes the depth of particle immersion in metallic phase.

From (12) the dependence of Q_k on inter-particle distance may be expressed through the change of meniscus elevation h_k:

$$\frac{dQ_k}{dL} = -\frac{1}{2} \cdot q^2 \cdot r_k^2 \cdot \frac{dh_k}{dL}. \tag{13}$$

The inter-particle attractive or repulsive force F results from the system energy:

$$F = \frac{d(\Delta W)}{dL} \tag{14}$$

$$\Delta W = W - W_\infty. \tag{15}$$

Thus the energy is related to its value at infinite inter-particle distance, where the interaction force F is zero. After necessary rearrangements N a k a j i m a and M i z o g u c h i [3] arrive at the relations between particular energy components and the elevation of meniscus h_k:

$$\frac{d(\Delta W)_g}{dL} = -\pi \cdot \gamma \cdot \sum_{k=1}^{2} 2 \cdot Q_k \cdot \frac{dh_k}{dL} \tag{16}$$

$$\frac{d(\Delta W)_w}{dL} = -\pi \cdot \gamma \cdot \sum_{k=1}^{2} \left[(q \cdot r_k)^2 \cdot R_k \cdot \cos\alpha_k\right] \cdot \frac{dh_k}{dL} \tag{17}$$

$$\frac{d(\Delta W)_m}{dL} = \pi \cdot \gamma \cdot \sum_{k=1}^{2} \left[Q_k + (q \cdot r_k)^2 \cdot R_k \cdot \cos\alpha_k\right] \cdot \frac{dh_k}{dL} \tag{18}$$

It follows from (1) and (16-18), that:

$$\frac{d(\Delta W)}{dL} = -\pi \cdot \gamma \cdot \sum_{k=1}^{2} Q_k \cdot \frac{dh_k}{dL} \tag{19}$$

It should be noticed that the net value of inter-particle force (19) is a half of the force resulting from gravitational energy (16).

In order to calculate the inter-particle force the relation is necessary between the elevation of meniscus h_k at three-phase line and the inter-particle distance L. The approximate solution to this problem based on the linearization of Laplace equation for $(q \cdot R_k)^2 << 1$ was given by P a u n o w, K r a l c h e v s k y et al. [6, 7] and is presented in equations (27-32). These dependences are used in subsequent calculations.

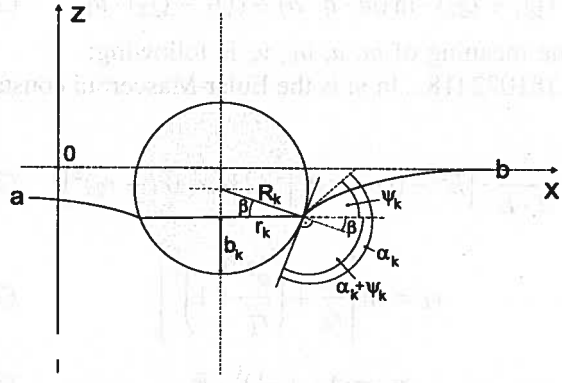

Fig. 2. Scheme for calculation of the radius of three-phase line r_k and immersion depth b_k. Line a-b marks the section of metal-slag interface

Basic geometric relations may be deduced from Fig. 2. If the angle of meniscus slope is low, the three-phase contact line may be assumed horizontal and the radius of contact line as well as immersion depth may be expressed as:

$$r_k = R_k \cdot \cos\beta, \tag{20}$$

where:

$$\beta = (\alpha_k + \psi_k) - \frac{\pi}{2}. \tag{21}$$

Thus

$$r_k = R_k \cdot \sin(\alpha_k + \psi_k) \tag{22}$$

The depth of particle immersion in metal is determined as

$$\begin{aligned} b_k &= R_k - R_k \cdot \sin\beta = R_k \cdot (1 - \sin\beta) = \\ &= R_k \cdot [1 + \cos(\alpha_k + \psi_k)]. \end{aligned} \tag{23}$$

Under assumption of small value of ψ_k ($\cos\psi_k \approx 1$) equation (22) may be presented as:

$$\begin{aligned} r_k &= R_k \cdot \sin(\alpha_k + \psi_k) = \\ &= R_k \cdot \cos\alpha_k \cdot \sin\psi_k + R_k \cdot \sin\alpha_k. \end{aligned} \tag{24}$$

Introduction of (11) leads to the quadratic equation:

$$r_k^2 - R_k \cdot \sin\alpha_k \cdot r_k - R_k \cdot Q_k \cdot \cos\alpha_k = 0. \tag{25}$$

From (25) the radius of three-phase contact line may be expressed as:

$$r_k = \frac{1}{2} \cdot \left[R_k \cdot \sin\alpha_k + \left(R_k^2 \cdot \sin^2\alpha_k + 4 \cdot Q_k \cdot R_k \cdot \cos\alpha_k\right)^{\frac{1}{2}}\right]. \tag{26}$$

The elevation of contact line for small particles is expressed as:

$$\begin{aligned} h_k &= Q_k \cdot \{v_k + 2 \cdot \ln[1 - \exp(-2 \cdot v_k)]\} - \\ &- (Q_1 + Q_2) \cdot \ln(m \cdot q \cdot a) + (Q_1 - Q_2) \cdot u_k. \end{aligned} \tag{27}$$

The meaning of m, a, u_k, v_k is following:
$m = 1.781072418...$ ln m is the Euler-Masceroni constant

$$a = \frac{1}{2 \cdot L} \cdot \left[L^2 - (r_1 + r_2)^2\right]^{\frac{1}{2}} \cdot \left[L^2 - (r_1 - r_2)^2\right]^{\frac{1}{2}} \tag{28}$$

$$v_k = \ln\left[\frac{a}{r_k} + \left(\frac{a^2}{r_k^2} + 1\right)^{\frac{1}{2}}\right] \tag{29}$$

$$u_k = A - (-1)^k \cdot B \tag{30}$$

$$A = \sum_{n=1}^{\infty} \frac{1}{n} \cdot \frac{\sinh n \cdot (v_1 - v_2)}{\sinh n \cdot (v_1 + v_2)} \tag{31}$$

$$B = \sum_{n=1}^{\infty} \frac{2}{n} \cdot \frac{\exp[-n \cdot v_k \cdot \sinh n \cdot v_l]}{\sinh n \cdot (v_1 + v_2)} \; k, l = 1, 2 \; k \neq l \tag{32}$$

3. Calculations procedure

The following iterative procedure, similar to this presented in [3] and [6] was applied in the calculations:

1. Starting values (indexed "0") are calculated for infinite separation between particles (single particle) from the following relations:

$$\begin{aligned} Q_k^{(0)} = Q_{k\infty} &= \frac{1}{6} \cdot q^2 \cdot R_k^3 \cdot \\ &\cdot \left(2 - 4 \cdot D_k + 3 \cdot \cos\alpha_k - (\cos\alpha_k)^3\right) \end{aligned} \tag{33}$$

$r_k^{(0)} = r_{k\infty}$ is calculated from eqn. (26) using the above value of $Q_k^{(0)}$.

With the above values of $Q_k^{(0)}$ and $r_k^{(0)}$, $\psi_k^{(0)} = \psi_{k\infty}$ is calculated from eqn. (11).

Next $b_k^{(0)} = b_{k\infty}$ is calculated from eqn. (23).

Contact line elevation at infinite separation is calculated by means of eqn. (34) from [3]:

$$\begin{aligned} h_k^{(0)} = h_{k\infty} &= r_{k\infty} \cdot \sin\psi_{k\infty} \cdot \\ &\cdot \ln\frac{4}{m \cdot q \cdot r_{k\infty} \cdot (1 + \cos\psi_{k\infty})}. \end{aligned} \tag{34}$$

2. Substitution: $Q_k = Q_k^{(n)}$ and $r_k = r_k^{(n)}$ and calculation of the value $h_k^{(n+1)}$ from (27)–(32).

The next approximation of $Q_k^{(n+1)}$ is obtained from eqn. (13) in the form:

$$Q_k^{(n+1)} = Q_k^{(n)} - \frac{1}{2} \cdot q^2 \cdot r_k^2 \cdot \left[h_k^{(n+1)} - h_k^{(n)}\right]. \tag{35}$$

Next the value of $r_k^{(n+1)}$ is calculated from eqn. (26).

The procedure presented here is quickly converged.

It should be noted that calculations are initiated for single (separated) particles. The link between both particles geometric parameters is obtained through eqn. (27).

3. Finally the inter-particle force is calculated from eqn. (36)

$$F = 2\pi \cdot \gamma \cdot \frac{Q_1 \cdot Q_2}{L}, \tag{36}$$

which is the reduced form of (19) for $(q \cdot L)^2 << 1$.

4. Results of calculations

The results of calculations are presented in Figs. 3-8. Fig. 3 shows the comparison of the values of attractive forces calculated for various radii of particles placed at the metal-gas and metal-slag interfaces. The

forces obtained for steel surface without slag are at least one order of magnitude higher than these for metal-slag interface. The attractive force depends also on the value of metal-slag interfacial tension and the dimensions of particles. These trends may be summarized as follows:

- Higher metal-slag interfacial tension results in weaker attractive force.
- Bigger particles exert stronger interaction.
- Particles of equal dimensions act more strongly on each other, than particles of different dimensions.

In all cases under consideration the typical shape of attractive force vs. inter-particle distance is preserved.

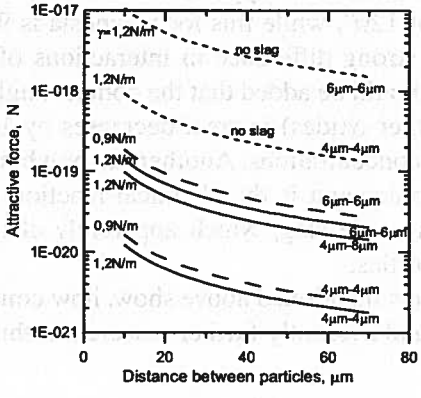

Fig. 3. Calculated capillary forces acting between particles of different radii at the surface of liquid steel with and without slag: $\rho_1 = \rho_2 = 3600$ kg/m^3, $\rho_m = 7000$ kg/m^3, $\rho_s = 3000$ kg/m^3, $\alpha = 135^0$

The calculated values of capillary forces acting at different distances were presented in Fig. 4, for selected values of contact angle. The force obviously decreases with the inter-particle distance. However, the dependence on contact angle is more complicated. For contact angle 125^0 the attraction is weaker by the factor of more than 10 in comparison with the angles 110 and 135^0.

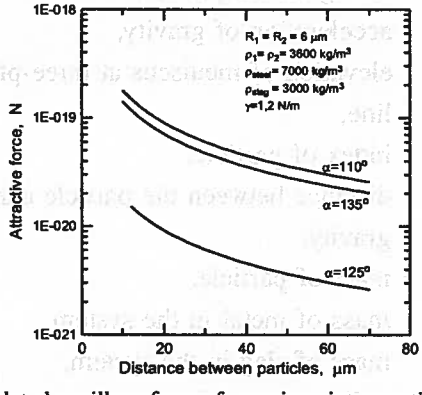

Fig. 4. Calculated capillary forces for various inter-particle distances and selected values of contact angle

Fig. 5 and 6 presents the influence of contact angle on the capillary force for inter-particle separation 40 μm. Sharp minimum may be noticed for the contact angle 120^0 if the slag density is 3000 kg/m^3 and 110^0 if the slag density is 2400 kg/m^3. In both cases this minimum is very deep (4-5 orders of magnitude).

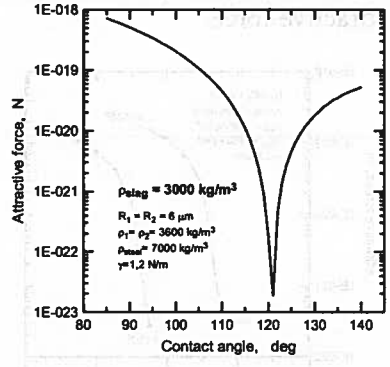

Fig. 5. Influence of contact angle on capillary force for inter-particle distance 40 μm; slag density 3000 kg/m^3

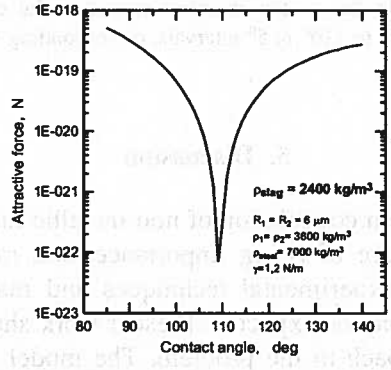

Fig. 6. Influence of contact angle on capillary force for inter-particle distance 40 μm; slag density 2400 kg/m^3

Fig. 7 shows, how the attractive force falls with increasing density of slag. If the slag density approaches this of solid particles, they are in fact suspended in the slag and the metal-slag interface deformation is negligible.

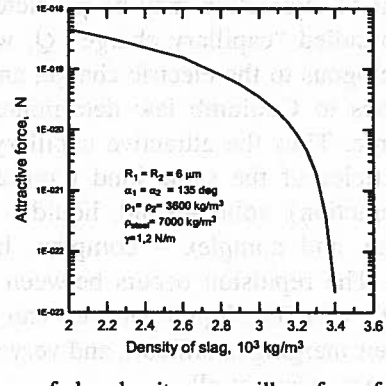

Fig. 7. Influence of slag density on capillary force for inter-particle distance 40 μm

Fig. 8 presents the variation of attraction force in the hypothetical process, in which approaching the particles

corresponds to the reduction of contact angle due to the chemical reaction. The contact angle varies from 135^0 to 110^0 in 5^0 intervals, corresponding to equal time intervals. It is evident, that transformation of Al_2O_3 particles into Al_2O_3-MgO or Al_2O_3-SiO_2 is accompanied with the decrease of attractive force.

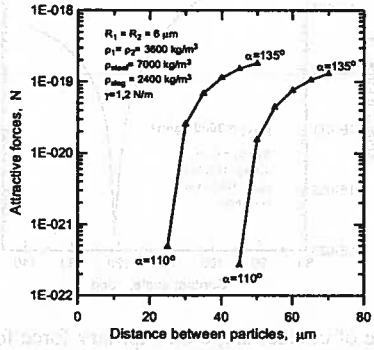

Fig. 8. The variation of attraction force in the hypothetical process, in which approaching of the particles corresponds to the reduction of contact angle due to the chemical reaction. The contact angle varies from 135^0 to 110^0 in 5^0 intervals, corresponding to equal time intervals

5. Discussion

Studies on coagulation of non-metallic inclusions in liquid steel are of rising importance, and rapid development on experimental techniques and mathematical modelling may be expected. Present work shows a simplified approach to the problem. The model of particle interactions adopted in the present work assumes, that particles do not undergo external forces, what is not the case in the actual conditions in metallurgical reactors. However, the dimensions of two-particle system under consideration (ca 100 μm) are small in comparison to the average size of turbulent vortices in steel, so it may be assumed that the velocity field acts on both particles in the same way.

The sign of interaction may be predicted from the values of so called "capillary charge" Q, which is the property analogous to the electric charge, and the equation analogous to Coulomb law determines the value of acting force. Thus the attractive capillary forces act between particles of the same kind (contrary to electrostatic interaction): solid – solid, liquid – liquid, solid – complex and complex – complex. In this case $Q1 \cdot Q2 > 0$. The repulsion occurs between unlike particles ($Q1 \cdot Q2 < 0$). The liquid particles can attract each other, but their merging is difficult, and very small liquid particles do not merge at all.

Another assumption in the present calculations regards the spherical shape of particles. In the course of coagulation the cluster shapes with tips are frequently observed, especially in the case of alumina. To extend calculations on the particles of complex geometry (network-like or coral-like) the shape conversion factor has to be applied [3].

The calculations in the present work are based on the selected typical values of density of slag and oxide inclusions, the interface tension and contact angle. Due to the lack of appropriate experimental data the values used in calculations can not be attributed to any specific temperature and combination of slag and inclusion compositions. However, these values locate in the range of real materials properties.

It is clear from the presented results of calculations that contact angle is very important factor in inter-particle attraction. Typical contact angle for alumina is about 120^0, while this for magnesia is 90^0. This explains the strong difference in interactions of various particles. It should be added that the contact angle of alumina (and other oxides) in steel decreases by $10\text{-}30^0$ at high oxygen concentrations. Another factor which should be taken into account is the chemical reaction of oxide particle with oxide slag, which apparently changes the surface properties.

The effects mentioned above show, how complex the problem is, and evidently further research in this field is necessary.

List of symbols:

A_{k-m} – area of particle – metal contact surface,
A_{k-s} – area of particle – slag contact surface,
b_k – the depth of particle immersion in metallic phase,
D_k – density factor,
F – inter-particle attractive ore repulsive force,
F_k^g – the gravity force (including buoyancy) acting on the particle,
g – acceleration of gravity,
h_k – elevation of meniscus at three-phase contact line,
k – index of particle,
L – distance between the particle centres of gravity,
m_k – mass of particle,
m_m – mass of metal in the system,
m_s – mass of slag in the system,
R_k – radius of particle,
r_k – horizontal radius of three-phase contact line,
V_k^m – part of particle volume submerged in metal,
V_k^s – part of particle volume submerged in slag,

V_k – total volume of particle,
z_k^0 – elevation of particle centre of gravity,
z_m^0 – elevation of metal centre of gravity,
z_s^0 – elevation of slag centre of gravity,
α_k – three-phase contact angle,
γ – slag-metal interfacial tension,
ρ_k – density of particle material,
ρ_m – density of liquid metal (steel),
ρ_s – density of liquid slag,
ψ_k – angle of meniscus slope at the contact line,
ω_{k-m} – surface energy density (interfacial tension) particle – metal,
ω_{k-s} – surface energy density particle – slag.

Acknowledgements

This work was financed by the Polish State Committee for Scientific Research in the year 2004 - project nr 3 T08B 011 26.

Received: 17 May 2005.

REFERENCES

[1] H. Yin, H. Shibata, T. Emi, M. Suzuki, ISIJ Intern. **37**, 936-945 (1997).
[2] H. Yin, H. Shibata, T. Emi, M. Suzuki, ISIJ Intern. **37**, 946-955 (1997).
[3] K. Nakajima, S. Mizoguchi, Metall. and Materials Trans. B **32B**, 629-641 (2001).
[4] B. Coletti, S. Vantilt, B. Blanpain, S. Sridhar, Metall. and Materials Trans. B **34B**, 533-538 (2003).
[5] S. Vantilt, B. Coletti, B. Blanpain, J. Fransaer, P. Wollants, S. Sridhar, ISIJ Int. **44**, 1-10 (2004).
[6] V. Paunov, P. Kralchevsky, N. Denkov, K. Nagayama, J. Colloid and Interface Sc. **157**, 100-112 (1993).
[7] P. Kralchevsky, N. Denkov, V. Paunov, O. Velev, I. Ivanov, H. Yoshimura, K. Nagayama, J. Phys. Cond. Matter **6**, A395-A402 (1994).